Available online at www.sciencedirect.com
SCIENCE DIRECT
International Journal of Heat and Mass Transfer 49 (2006) 3595–3600
International Journal of HEAT and MASS TRANSFER
www.elsevier.com/locate/ijhmt

Numerical simulation of the natural convection plume about line heat source in micropolar fluid

Cheng-Long Chang *

Department of Mechanical Engineering, Hsiuping Institute of Technology, Dali, Taichung 412, Taiwan, ROC

Received 31 January 2005
Available online 19 April 2006

Abstract

This paper analyses the flow and heat transfer characteristics of laminar free convection in the boundary layer flow of micropolar fluids about a line heat source embedded on the edge of a plate. The nonlinear formulation governing equations are initially cast into dimensionless form by a local non-similar transformation and the resulting system of equations is then solved by the cubic spline collocation method and the finite difference scheme. Of particular interest are the effects of the micropolar parameter, Δ, and the Prandtl number on the velocity and temperature fields and on the skin friction coefficient, wall couple stress, and wall temperature. Numerical results are obtained for the velocity and temperature profiles for different values of the Prandtl number and micropolar parameter.

Keywords: Micropolar fluid; Line heat source; Natural convection

1. Introduction

The problem of natural convection flow around a concentrated heat source has been studied extensively by many investigators since this problem is of fundamental interest in many practical technological applications. Line heat sources are frequently used in a variety of applications, including in geophysical flows, the cooling of electronic circuitry, hot-wire anemometry, and heat treatment processing.

Early experimental studies performed by Schorr [1], Hieber and Nash [2], and Yosinobu et al. [3] obtained results for laminar free convection around a horizontal line heat source. Later, Gebhar et al. [4] and Fujii et al. [5] investigated the natural convection plumes occurring above a horizontal line heat source via numerical computations of similarity solutions. Similarly, Jaluria and Gebhar [6] also used similarity solutions to solve the flow caused by a line heat source at the edge of a wall. Their results indicated that the wall temperature decays along the vertical distance above the heat source. The vertical wall plume generated by a line heat source embedded on the leading edge of an adiabatic vertical plate has been studied extensively by Sparrow et al. [7] and Afzal [8]. Rao et al. [9] and Lin and Chen [10] used numerical methods to analyze the mixed convection wall plumes formed between the forced convection limit and the free convection limit of fluids.

An analysis of inclined and horizontal wall plumes has been conducted by Lin et al. [11] using both theoretical and experimental methods. Higuera and Weidman [12] considered the interaction between the plume and various surfaces and derived the corresponding formulation models. Recently, the problem of transient natural convection in liquid nitrogen around a heated wire has been solved experimentally and numerically by Duluc et al. [13]. Dias Jr. and Milanez [14] adopted two- and three-dimensional formulations to study the flow over a heat source mounted flush on a vertical adiabatic surface. Their results established the existence of a transition between the two- and three-dimensional plumes.

The investigations cited above all considered the fluid to be Newtonian. However, in practice, many of the fluids

* Tel.: +886 4 249 61100; fax: +886 4 2496 1188.
E-mail address: clchang@mail.hit.edu.tw

0017-9310/$ - see front matter © 2006 Elsevier Ltd. All rights reserved.
doi:10.1016/j.ijheatmasstransfer.2006.02.040

involved in technical processes and engineering applications exhibit non-Newtonian behavior. Consequently, it is necessary to extend the analysis of natural convection plumes to the case of non-Newtonian fluids. The theory of micropolar fluids was first developed by Eringen [15] and has been applied to the investigation of various fluids. This theory takes the microscopic effects arising from the local structure and micro-motions of the fluid elements into account and provides the basis for a mathematical model for non-Newtonian fluids which can be used to analyze the behavior of exotic lubricants, polymers, liquid crystals, animal bloods, and colloidal or suspension solutions, etc. Eringen [16] later extended this theory to the investigation of thermo-micropolar fluids by taking thermal effects into account. A comprehensive review of micropolar fluids theory and the application of micropolar fluid mechanics has been presented by Ariman et al. [17]. Ahmadi [18] obtained a similarity solution for the micropolar boundary layer flow over a semi-infinite plate. The problem of free convection heat transfer in the boundary layer flow along a vertical or horizontal surface submerged in a micropolar fluid has been extensively studied by a number of investigators [19–22].

A review of the published literature reveals that the problem of laminar natural convection wall plumes in a micropolar fluid has yet to be reported. However, this problem is of great significance in many industrial and theoretical applications, and therefore merits thorough investigation. Consequently, the present study applies the cubic spline collocation method and the finite difference approximation scheme to investigate the nonlinear system of this particular problem. The effects of the micropolar parameter, the Prandtl number, and the heat characteristics are considered. Additionally, a comparison is performed between the present results for the wall temperature and wall friction and the numerical results presented previously [10] for the pure free convection of a Newtonian fluid wall plume. It is shown that the two sets of results are in good agreement.

2. Mathematical formulation

Consider the steady laminar natural convection of a micropolar fluid flow over a vertical plate with a line heat source embedded in its leading edge, constantly generating heat at a rate of Q. The corresponding physical model and coordinate system are shown in Fig. 1. The x-coordinate is measured along the wall and the y-coordinate is measured normally from the wall. The gravitational acceleration, g, acts in the downward direction. Other than the density variation, the remaining fluid properties are assumed to be constant. It is noted that the temperature difference between the body surface and the surrounding micropolar fluid causes a buoyancy force which results in an upward convective flow. The viscous dissipation is considered to be negligible.

By employing laminar boundary layer flow assumptions and the Boussinesq approximation, the governing conservation equations for the micropolar fluid can be written as

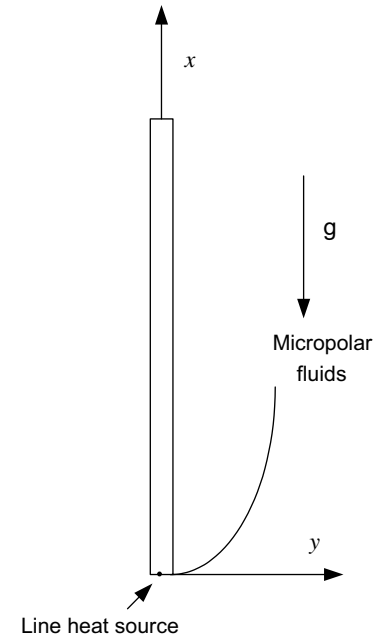

Fig. 1. Physical model and coordinate system.

For continuity,

$$\frac{\partial u}{\partial x}+\frac{\partial v}{\partial y}=0. \tag{1}$$

For momentum,

$$u\frac{\partial u}{\partial x}+v\frac{\partial u}{\partial y}=\left(\nu+\frac{\kappa}{\rho}\right)\frac{\partial^2 u}{\partial y^2}+\frac{\kappa}{\rho}\frac{\partial N}{\partial y}+g\beta(T-T_\infty). \tag{2}$$

For angular momentum,

$$u\frac{\partial N}{\partial x}+v\frac{\partial N}{\partial y}=\frac{\gamma}{j\rho}\frac{\partial^2 N}{\partial y^2}-\frac{\kappa}{j\rho}\left(\frac{\partial u}{\partial y}+2N\right). \tag{3}$$

For energy,

$$u\frac{\partial T}{\partial x}+v\frac{\partial T}{\partial y}=\alpha\frac{\partial^2 T}{\partial y^2}. \tag{4}$$

In these equations, u and v are the velocity components along the x- and y-directions, respectively, ρ, ν, α, and β are the density, kinematic viscosity, thermal diffusivity, and thermal expansion coefficient of the fluid, respectively, and κ, j, and γ are the vortex viscosity, micro-inertia density, and spin-gradient viscosity of the fluid, respectively. Finally, T is the fluid temperature and N is the component of micro-rotation whose direction of rotation lies in the (x–y) plane.

The boundary conditions are given by the following:

$$y=0: u=0,\quad v=0,\quad N=-\frac{1}{2}\frac{\partial u}{\partial y},\quad \frac{\partial T}{\partial y}=0, \tag{5a}$$

$$y\to\infty: u=0,\quad N=0,\quad T=T_\infty. \tag{5b}$$

In general, the boundary condition given in (5a) for N at the plate, i.e. $y=0$, may express $N=-n(\partial u/\partial y)$. The physical interpretation is that there is a strong concentration of

micro-elements in the vicinity of boundary for $n = 0$, a turbulent boundary layer for $n = 1$, and a weak concentration at the wall for $n = 1/2$ as suggested by Ahmadi [18] and Gorla and Ameri [20] indicates that the micro-rotation is equal to one half of the fluid vorticity at the boundary. In this paper, we have limited to the case of $n = 1/2$ only.

In addition, the convective energy carried by the boundary layer flow is equal to the energy released by the line heat source. Therefore, it follows that:

$$Q = \rho C_p L \int_0^\infty u(T - T_\infty)\,\mathrm{d}y \tag{6}$$

where C_p and L are the specific heat of the fluid and the length of the line heat source, respectively.

To facilitate the solution of the current problem, this paper introduces the pseudo similarity variables ξ and η, the reduced stream function $F(\xi,\eta)$, the dimensionless micro-rotation $G(\xi,\eta)$, and the dimensionless temperature, i.e.

$$\begin{aligned} &\xi = \frac{x}{L}, \quad \eta = \frac{y}{L\xi^{2/5}}Gr^{1/5}, \quad F(\xi,\eta) = \frac{1}{\nu Gr^{1/5}\xi^{3/5}}\varphi, \\ &G(\xi,\eta) = \frac{L^2\xi^{1/5}}{\nu Gr^{3/5}}N, \quad \theta(\xi,\eta) = \frac{T - T_\infty}{T^*}Gr^{1/5}\xi^{3/5}, \end{aligned} \tag{7}$$

where Gr is the Grashof number, i.e.

$$Gr = g\beta T^* L^3/\nu^2 \tag{8}$$

and T^* is the characteristic temperature of the line heat source, i.e.

$$T^* = \frac{Q}{\rho C_p \nu L}. \tag{9}$$

The stream function, φ, satisfies the continuity equation given in Eq. (1) automatically with

$$u = \frac{\partial\varphi}{\partial y}, \quad v = -\frac{\partial\varphi}{\partial x}. \tag{10}$$

Substituting Eq. (7) into the governing equation (2)–(4) and (6), respectively, leads to

$$\begin{aligned} &(1+\Delta)F''' + \frac{3}{5}FF'' - \frac{1}{5}F'F' + \Delta G' + \theta \\ &\quad = \xi\left(F'\frac{\partial F'}{\partial\xi} - F''\frac{\partial F}{\partial\xi}\right), \end{aligned} \tag{11}$$

$$\begin{aligned} &\lambda G'' + \frac{3}{5}FG' + \frac{1}{5}F'G - \Delta B\xi^{4/5}(2G + F'') \\ &\quad = \xi\left(F'\frac{\partial G}{\partial\xi} - G'\frac{\partial F}{\partial\xi}\right), \end{aligned} \tag{12}$$

$$\frac{1}{Pr}\theta'' + \frac{3}{5}F\theta' + \frac{3}{5}F'\theta = \xi\left(F'\frac{\partial\theta}{\partial\xi} - \theta'\frac{\partial F}{\partial\xi}\right), \tag{13}$$

$$\int_0^\infty F'\theta\,\mathrm{d}\eta = 1. \tag{14}$$

In the equations above, the primes indicate partial differentiation with respect to η alone and $Pr = \nu/\alpha$ is the Prandtl number. Meanwhile, the dimensionless parameters Δ, B, and λ characterize the vortex viscosity, the micro-inertia density, and the spin-gradient viscosity, respectively, and are defined as

$$\Delta = \frac{\kappa}{\mu}, \quad B = \frac{L^2}{jGr^{2/5}}, \quad \lambda = \frac{\gamma}{j\rho\nu}.$$

Following transformation, the corresponding boundary conditions, Eqs. (5a) and (5b), become

At $\eta = 0$:

$$\begin{aligned} &F'(\xi,0) = 0, \quad F(\xi,0) = -\frac{5}{3}\xi\left.\frac{\partial F}{\partial\xi}\right|_{\eta=0}, \\ &G(\xi,0) = -\frac{1}{2}F''(\xi,0), \quad \theta'(\xi,0) = 0. \end{aligned} \tag{15a}$$

At $y \to \infty$:

$$F'(\xi,\infty) = G(\xi,\infty) = \theta(\xi,\infty) = 0. \tag{15b}$$

It is noted that for the limiting case of $\Delta = 0$, the fluid becomes a Newtonian fluid, and Eqs. (11) and (13), which govern the micropolar fluid flow, reduce to the pure free convection case of [10]. In this case, Eq. (12) has no significance and can be omitted.

In the natural convection flow of micropolar fluids, the physical quantities of principal interest are the wall temperature distribution, $\theta(\xi,0)$, the skin friction coefficient, C_f, the dimensionless wall couple stress, M_w, the velocity distribution, F', and the micro-rotation distribution, G. The first three quantities are defined, respectively, by

$$\frac{T_w - T_\infty}{T^*}Gr^{1/5} = \xi^{-3/5}\theta(\xi,0), \tag{16}$$

$$C_f = \frac{2\tau_w}{\rho U_*^2}, \tag{17}$$

$$M_w = \frac{m_w}{\rho U_*^2 L}, \tag{18}$$

where $U_* = \nu Gr^{2/5}\xi^{1/5}/L$ is the characteristic velocity.

With the aid of Eq. (7), together with a definition of the wall shear stress as $\tau_w = [(\mu+\kappa)\frac{\partial u}{\partial y} + \kappa N]_{y=0}$, and the wall couple stress as $m_w = \gamma\left.\frac{\partial N}{\partial y}\right|_{y=0}$, it can be shown that

$$C_f Gr^{1/5} = 2\left(1 + \frac{\Delta}{2}\right)\xi^{-3/5}F''(\xi,0), \tag{19}$$

$$M_w Gr^{2/5} = \frac{\lambda}{B}\xi^{-1}G'(\xi,0). \tag{20}$$

2.1. Numerical procedure

To solve the current problem, the system of nonlinear equations given in Eqs. (11)–(14) and the associated boundary conditions in Eq. (15) must be solved simultaneously due to the coupled nature of the system. The solution of the system of steady equations has been obtained previously using a pseudo-transient formulation approach in which a false transient term was introduced into each equation [23,24]. The present study solves the coupled nonlinear partial differential equations using the cubic spline

collocation method [23–26] together with a finite difference approximation. The principal advantages of using the cubic spline collocation technique are reported in [23,26] and are not repeated here.

Using the false transient technique, Eqs. (11)–(13) can be expressed in discretized form as

$$\frac{u_{i,j}^{n+1}-u_{i,j}^{n}}{\Delta\tau}=(1+\Delta)L_{u_{i,j}}^{n+1}+\left(\frac{3}{5}F_{i,j}^{n}+\xi_i\frac{F_{i,j}^{n}-F_{i-1,j}^{n}}{\Delta\xi_i}\right)l_{u_{i,j}}^{n+1}+\Delta l_{G_{i,j}}^{n}+\theta_{i,j}^{n+1}-\frac{1}{5}u_{i,j}^{n}u_{i,j}^{n}-\xi_i u_{i,j}^{n}\frac{u_{i,j}^{n}-u_{i-1,j}^{n}}{\Delta\xi_i}, \quad (21)$$

$$\frac{G_{i,j}^{n+1}-G_{i,j}^{n}}{\Delta\tau}=\lambda L_{G_{i,j}}^{n+1}+\left(\frac{3}{5}F_{i,j}^{n+1}+\xi_i\frac{F_{i,j}^{n+1}-F_{i-1,j}^{n+1}}{\Delta\xi_i}\right)l_{G_{i,j}}^{n+1}+\frac{1}{5}u_{i,j}^{n+1}G_{i,j}^{n}-\Delta B\xi_i^{4/5}(2G_{i,j}^{n}+l_{u_{i,j}}^{n+1})-\xi_i u_{i,j}^{n+1}\frac{G_{i,j}^{n}-G_{i-1,j}^{n}}{\Delta\xi_i}, \quad (22)$$

$$\frac{\theta_{i,j}^{n+1}-\theta_{i,j}^{n}}{\Delta\tau}=\frac{1}{Pr}L_{\theta_{i,j}}^{n+1}+\left(\frac{3}{5}F_{i,j}^{n}+\xi_i\frac{F_{i,j}^{n}-F_{i-1,j}^{n}}{\Delta\xi_i}\right)l_{\theta_{i,j}}^{n+1}+\frac{3}{5}u_{i,j}^{n}\theta_{i,j}^{n}-\xi_i u_{i,j}^{n}\frac{\theta_{i,j}^{n}-\theta_{i-1,j}^{n}}{\Delta\xi_i}, \quad (23)$$

where

$$l_u=\frac{\partial u}{\partial\eta},\quad L_u=\frac{\partial^2 u}{\partial\eta^2},\qquad l_G=\frac{\partial G}{\partial\eta},\quad L_G=\frac{\partial^2 G}{\partial\eta^2},\qquad l_\theta=\frac{\partial\theta}{\partial\eta},\quad L_\theta=\frac{\partial^2\theta}{\partial\eta^2},\qquad \Delta\xi_i=\xi_i-\xi_{i-1}. \quad (24)$$

In the above, $\Delta\tau=\tau^{n+1}-\tau^{n}$ represents the false time step, the subscript u indicates $\partial F/\partial\eta$, and the superscript n denotes the iteration order.

Following rearrangement, Eqs. (21)–(23) can be expressed in the following spline approximation form:

$$\phi_{i,j}^{n+1}=Q_{i,j}+R_{i,j}l_{\phi_{i,j}}^{n+1}+S_{i,j}L_{\phi_{i,j}}^{n+1}, \quad (25)$$

where ϕ represents the functions u, G, and θ. The quantities $Q_{i,j}$, $R_{i,j}$, and $S_{i,j}$, are known coefficients, calculated at previous time steps (Table 1).

In the present analysis, the cubic spline collocation method is used to generate an algorithm resulting in a single tridiagonal system containing either the function values at the grid points, the first derivatives, or the second derivatives only. Using the cubic spline relations described by Rubin and Khosla [25], Eq. (25) at the $n+1$th iteration can be written in the following tridiagonal form:

$$a_{i,j}\phi_{i,j-1}^{n+1}+b_{i,j}\phi_{i,j}^{n+1}+c_{i,j}\phi_{i,j+1}^{n+1}=d_{i,j}, \quad (26)$$

where ϕ represents the function (u, G, and θ) and its first and second order derivatives. Therefore, Eq. (26) can be readily solved by using the Thomas algorithm.

The present computational procedure commences by solving the energy equation, which provides the temperature field necessary for the solution of the reduced stream function equation. Solution of the transformed angular momentum equation for G then completes the procedure. This computation cycle is repeated until convergence is obtained. The criterion applied when assessing the convergence of the solutions is that the maximum relative change in all of the dependent variables should satisfy:

$$\frac{|\phi_{i,j}^{n+1}-\phi_{i,j}^{n}|_{\max}}{|\phi_{i,j}^{n}|_{\max}}<1\times10^{-7}. \quad (27)$$

3. Results and discussion

In the present study, which aims to develop an understanding of the flow and heat transfer characteristics in micropolar fluid flows about a wall plume, the various numerical computations were all performed using $B=1\times10^{6}$ and $\lambda=5.0$. The remaining parameters were specified within the following ranges: micropolar parameter $\Delta=0$–20.0; Prandtl number $Pr=0.73$–20.0.

To assess the accuracy of the cubic spline collocation method, the present results were compared with the published data [10] relating to the natural convection of Newtonian fluids (i.e. $\Delta=B=\lambda=0$). For different values of Pr, the current results for the dimensionless wall temperature, $\theta(\xi,0)$, and the dimensionless wall friction coefficient, $F''(\xi,0)$, were found to be in good agreement with those of [10], as shown in Table 2.

Representative velocity profiles for various values of Δ are illustrated in Fig. 2, which plots F' against η for $Pr=9.0$ and 0.73, respectively. It can be seen that an increase in the micropolar parameter, Δ, causes a reduction in the maximum velocity ($F'_{\max}$) in the boundary layer. Additionally, it is observed that the larger the value of Δ,the thicker the momentum boundary layer. This observation is reasonable since an increase in Δ will increase the concentration of micro-elements near the boundary and

Table 1
Coefficients of Eq. (25)

ϕ	Q	R	S
u	$\Delta\tau\left(-\frac{1}{5}u_{i,j}^{n}u_{i,j}^{n}+\Delta l_{G_{i,j}}^{n}+\theta_{i,j}^{n+1}-\xi_i u_{i,j}^{n}\frac{u_{i,j}^{n}-u_{i-1,j}^{n}}{\Delta\xi_i}\right)+u_{i,j}^{n}$	$\Delta\tau\left(\frac{3}{5}F_{i,j}^{n}+\xi_i\frac{F_{i,j}^{n}-F_{i-1,j}^{n}}{\Delta\xi_i}\right)$	$\Delta\tau(1+\Delta)$
G	$\Delta\tau\left[\frac{1}{5}u_{i,j}^{n+1}G_{i,j}^{n}-\Delta B\xi^{4/5}(2G_{i,j}^{n}+l_{u_{i,j}}^{n+1})-\xi_i u_{i,j}^{n+1}\frac{G_{i,j}^{n}-G_{i-1,j}^{n}}{\Delta\xi_i}\right]+G_{i,j}^{n}$	$\Delta\tau\left(\frac{3}{5}F_{i,j}^{n+1}+\xi_i\frac{F_{i,j}^{n+1}-F_{i-1,j}^{n+1}}{\Delta\xi_i}\right)$	$\Delta\tau\lambda$
θ	$\Delta\tau\left(\frac{3}{5}\theta_{i,j}^{n}-\xi_i\frac{\theta_{i,j}^{n}-\theta_{i-1,j}^{n}}{\Delta\xi_i}\right)u_{i,j}^{n}+\theta_{i,j}^{n}$	$\Delta\tau\left(\frac{3}{5}F_{i,j}^{n}+\xi_i\frac{F_{i,j}^{n}-F_{i-1,j}^{n}}{\Delta\xi_i}\right)$	$\frac{\Delta\tau}{Pr}$

Table 2
Comparison of local wall temperature and skin friction coefficient

Pr	$\theta(\xi,0)$		$F''(\xi,0)$	
	Lin and Chen [10]	Present results	Lin and Chen [10]	Present results
0.001	0.79334	0.79487	52.114	52.301
0.01	0.79202	0.79254	15.585	15.597
0.1	0.77996	0.78018	4.5362	4.5375
0.7	0.73450	0.73446	1.8562	1.8563
7.0	0.65331	0.65256	1.2033	1.2035
100	0.60188	0.60207	1.1602	1.1608

will consequently cause the momentum boundary layer to become thicker.

Fig. 3 shows representative dimensionless temperature profiles for different values of Δ. An inspection of these profiles reveals that as the micropolar parameter, Δ, increases, both the temperature and the thermal boundary layer thickness increase. These trends are again attributed to the fact that a larger value of Δ leads to a higher concentration of micro-elements near the boundary.

The results of Table 3 demonstrate the effect of the micropolar parameter, Δ, on the skin friction parameter,

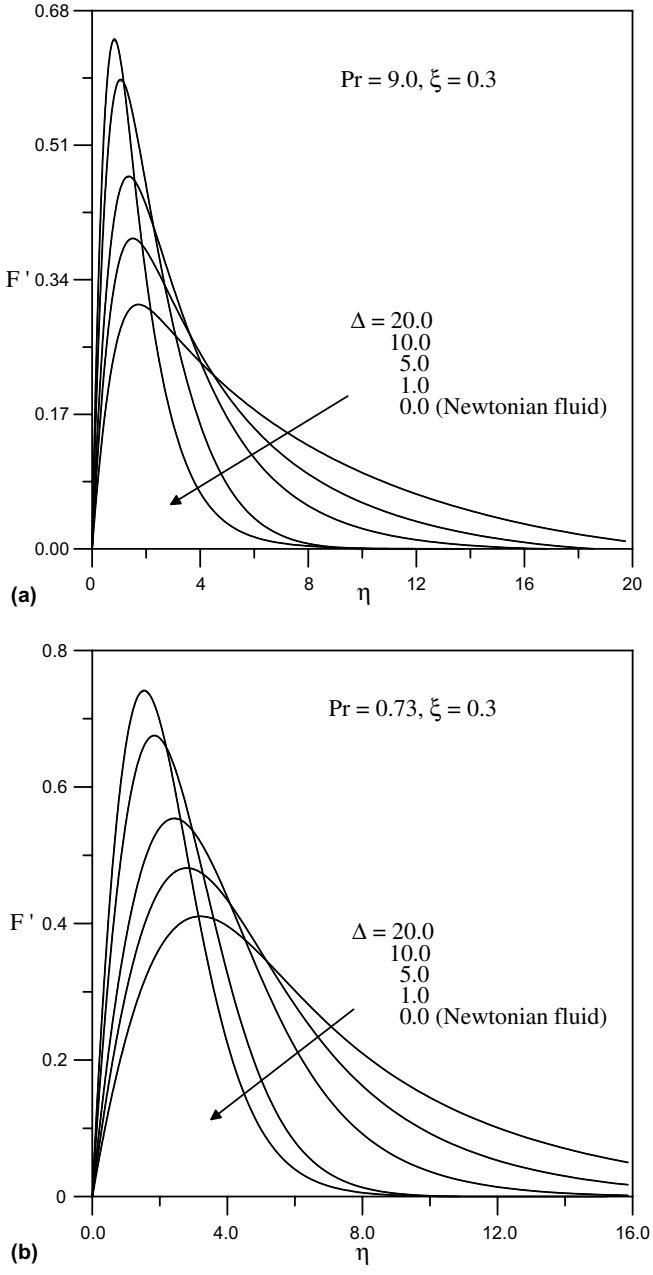

Fig. 2. Velocity profiles for selected values of Δ for $Pr = 9.0$, 0.73 and $\xi = 0.3$.

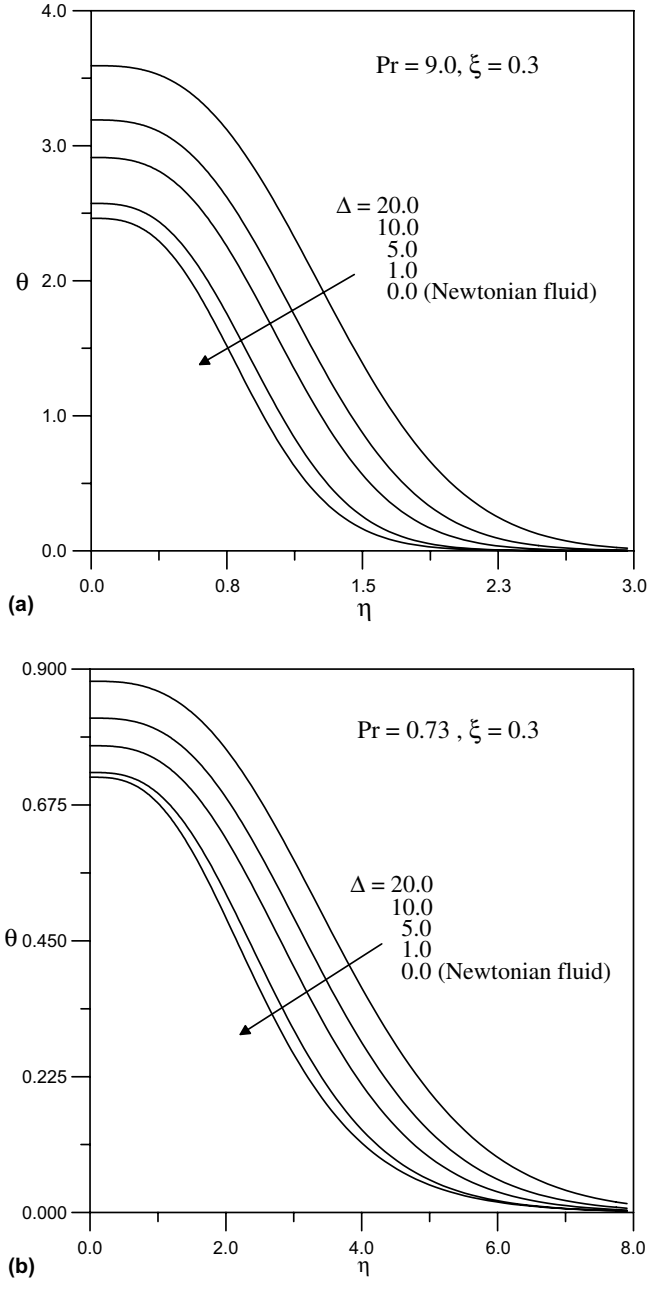

Fig. 3. Temperature profiles for selected values of Δ for $Pr = 9.0$ and $\xi = 0.3$.

Table 3
Effect of variation of Δ on skin friction parameter $F''(\xi,0)$, local wall temperature $\theta(\xi,0)$ and wall couple stress $G'(\xi,0)$ at wall surface, respectively, for $Pr = 0.73$, $\lambda = 5.0$, $B = 1\times10^6$, and $\xi = 0.1$

Δ	$F''(\xi,0)$	$\theta(\xi,0)$	$G'(\xi,0)$
0.0	1.02335	0.72107	–
0.5	0.86215	0.72316	0.27173
1.0	0.78320	0.72882	0.23421
2.0	0.66800	0.74169	0.18321
5.0	0.49453	0.77316	0.11588
10.0	0.37757	0.81893	0.07853
20.0	0.28633	0.87994	0.05346

Table 4
Effect of variation of Pr on local friction parameter $F''(\xi,0)$, local wall temperature $\theta(\xi,0)$ and wall couple stress $G'(\xi,0)$ at wall surface, respectively, for $\Delta = 1.0$, $\lambda = 5.0$, $B = 1\times10^6$, and $\xi = 0.1$

Pr	$F''(\xi,0)$	$\theta(\xi,0)$	$G'(\xi,0)$
0.01	0.30969	0.12576	0.04145
0.1	0.52864	0.31643	0.10342
0.73	0.78320	0.72882	0.23421
2.0	0.94821	1.17201	0.36236
9.0	1.28940	2.57325	0.75557
20.0	1.51086	4.00139	1.12418
90.0	2.06119	9.50491	2.58525

$F''(\xi,0)$, the dimensionless wall temperature, $\theta(\xi,0)$, and the dimensionless wall couple stress, $G'(\xi,0)$. It is observed that the skin friction parameter and the wall couple stress both decrease as Δ increases. This is because the boundary layer thicknesses of the momentum, thermal and angular velocity become thicker as the micropolar parameter Δ increases. The numerical results also indicate that the influence of vortex viscosity leads to the micropolar fluid ($\Delta \neq 0$) having a lower skin friction parameter and surface heat transfer rate than a Newtonian fluid $\Delta = 0$ under the same conditions.

Table 4 shows the effect of the Prandtl number, Pr, on the skin friction parameter, $F''(\xi,0)$, the wall temperature, $\theta(\xi,0)$, and the dimensionless wall couple stress, $G'(\xi,0)$. It is obvious that an increase in the Prandtl number causes a corresponding increase in the skin friction parameter, the wall temperature, and the wall couple stress.

4. Conclusions

This study has investigated the wall plume associated with natural convection flow in micropolar fluids. The numerical results for the transformed boundary layer equations with appropriate boundary conditions have been obtained using the cubic spline collocation method. The principal findings of this study can be summarized as follows:

(1) An increase in the micropolar parameter, Δ, causes a reduction in the maximum velocity ($F'_{\max}$) in the boundary layer and shifts the position of maximum velocity away from the surface. Meanwhile, the temperature in the boundary layer increases. Furthermore, higher values of Δ cause the thicknesses of the momentum and thermal boundary layers to increase.
(2) Both the skin friction parameter and the wall couple stress increase with increasing micropolar parameter, Δ. However, the local wall temperature decreases with increasing Δ.
(3) The micropolar parameter, Δ, has a significant influence on the velocity and temperature fields, and reduces the skin friction factor while increasing the local wall temperature compared to the case of Newtonian fluids ($\Delta = 0$).
(4) An increase in the Prandtl number, Pr, causes a corresponding increase in the skin friction parameter, the local wall temperature, and the wall couple stress.

References

[1] A.W. Schorr, Int. J. Heat Mass Transfer 13 (1970) 557.
[2] C.A. Hieber, E.J. Nash, Int. J. Heat Mass Transfer 18 (1975) 1473.
[3] H. Yosinobu, Y. Onishi, S. Amano, S. Enyo, S. Wakitani, J. Phys. Soc. Jpn. 47 (1) (1979) 312.
[4] B. Gebhart, L. Pera, A.W. Schorr, Int. J. Heat Mass Transfer 13 (1970) 161.
[5] T. Fujii, I. Morioka, H. Uehara, Int. J. Heat Mass Transfer 16 (1973) 755.
[6] Y. Jaluria, B. Gebhar, Int. J. Heat Mass Transfer 20 (1977) 153.
[7] E. Sparrow, S.V. Patankar, R.M. Abdul-Wahed, Trans. ASME J. Heat Transfer 100 (1978) 184.
[8] N. Afzal, Int. J. Heat Mass Transfer 23 (1980) 505.
[9] K.V. Rao, B.F. Armaly, T.S. Chen, Trans. ASME J. Heat Transfer 106 (1984) 552.
[10] H.T. Lin, J.J. Chen, Int. J. Heat Mass Transfer 30 (1987) 1721.
[11] H.T. Lin, J.J. Chen, L.W. Kung, W.S. Yu, Int. J. Heat Mass Transfer 39 (1996) 2243.
[12] F.J. Higuera, P.D. Weidman, Trans. ASME J. Fluid Mech. 361 (1998) 25.
[13] M.C. Duluc, S. Xin, P.L. Quere, Int. J. Heat Mass Transfer 46 (2003) 341.
[14] T. Dias Jr., L.F. Milanez, Int. J. Heat Mass Transfer 47 (2004) 1227.
[15] A.C. Eringen, Int. J. Eng. Sci. 2 (1964) 205.
[16] A.C. Eringen, J. Math. Anal. Appl. 38 (1972) 480.
[17] T. Ariman, M.A. Turk, N.D. Sylvester, Int. J. Eng. Sci. 11 (1973) 905.
[18] G. Ahmadi, Int. J. Eng. Sci. 14 (1976) 639.
[19] S.K. Jena, M.N. Mathur, Int. J. Eng. Sci. 19 (1981) 1431.
[20] R.S.R. Gorla, A. Ameri, Acta Mech. 57 (1985) 203.
[21] R.S.R. Gorla, Int. J. Eng. Sci. 23 (1985) 401.
[22] R.S.R. Gorla, H.S. Takhar, Int. J. Eng. Sci. 25 (1987) 949.
[23] M.I. Char, C.K. Chen, J.W. Cleaver, Int. J. Heat Fluid Flow 11 (1990) 257.
[24] S.G. Rubin, R.A. Graves, Comput. Fluids 3 (1975) 1.
[25] G.S. Rubin, P.K. Khosla, AIAA 14 (1976) 851.
[26] P. Wang, R. Kahawita, Int. J. Comput. Math. 13 (1983) 271.